NAR Cancer, 2024, **6**, zcae043
https://doi.org/10.1093/narcan/zcae043
Advance access publication date: 15 November 2024
Cancer Computational Biology

Integration of transcriptional and epigenetic regulation of TFEB reveals its dual functional roles in Pan-cancer

Jing-Fang Luo [1,2,3], Shijia Wang [2,3], Jiajing Fu [2,3], Peng Xu [4], Ningyi Shao [3,5,*], Jia-Hong Lu [1,*] and Chen Ming [2,3,6,*]

[1]State Key Laboratory of Quality Research in Chinese Medicine, Institute of Chinese Medical Sciences, University of Macau, Macao SAR 999078, China
[2]Department of Public Health and Medicinal Administration, Faculty of Health Sciences, University of Macau, Macao SAR 999078, China
[3]Ministry of Education Frontiers Science Centre for Precision Oncology, Faculty of Health Sciences, University of Macau, Macau SAR 999078, China
[4]Centre of Clinical Laboratory Medicine, Zhongda Hospital, School of Medicine, Advanced Institute for Life and Health, Southeast University, Nanjing 210096, China
[5]Department of Biomedical Sciences, Faculty of Health Sciences, University of Macau, Macao SAR 999078, China
[6]Centre for Cognitive and Brain Sciences, University of Macau, Macao SAR 999078, China

[*]To whom correspondence should be addressed. Tel: +853 8822 9117; Email: chenming@um.edu.mo
Correspondence may also be addressed to Jia-Hong Lu. Tel: +853 8822 4508; Email: jiahonglu@um.edu.mo
Correspondence may also be addressed to Ningyi Shao. Tel: +853 8822 4895; Email: nshao@um.edu.mo

Abstract

Transcription factor EB (TFEB) mainly regulates the autophagy-lysosomal pathway, associated with many diseases, including cancer. However, the role of TFEB in pan-cancer has not been investigated systematically. In this study, we comprehensively analyzed TFEB targets under three stresses in Hela cells by cross-validation of RNA-seq and ChIP-seq. 1712 novel TFEB targets have not been reported in the Gene Set Enrichment Analysis and ChIP Enrichment Analysis databases. We further investigated their distributions and roles among the pan-cancer co-expression networks across 32 cancers constructed by multiscale embedded gene co-expression network analysis (MEGENA) based on the Cancer Genome Atlas (TCGA) cohort. Specifically, TFEB might serve as a hidden player with multifaceted functions in regulating pan-cancer risk factors, e.g. *CXCL2*, *PKMYT1* and *BUB1*, associated with cell cycle and immunosuppression. TFEB might also regulate protective factors, e.g. *CD79A*, related to immune promotion in the tumor microenvironment. We further developed a Shiny app website to present the comprehensive regulatory targets of TFEB under various stimuli, intending to support further research on TFEB functions. Summarily, we provided references for the TFEB downstream targets responding to three stresses and the dual roles of TFEB and its targets in pan-cancer, which are promising anticancer targets that warrant further exploration.

Graphical abstract

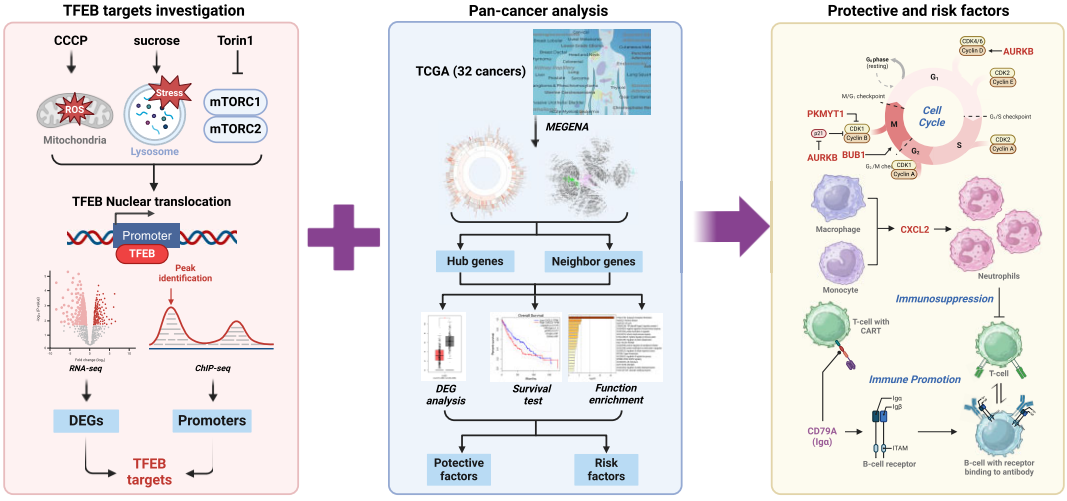

Received: August 14, 2024. **Revised:** October 3, 2024. **Editorial Decision:** October 21, 2024. **Accepted:** October 28, 2024

Introduction

Autophagy is a process of delivering cytoplasmic cargo to the lysosome for degradation, also named autophagy-lysosomal pathway (ALP). It is a critical intracellular degradation system for cleaning cellular components to support cell survival by responding to various stresses (1). Studies have found that it plays important dual roles in cancer development, progression, and prognosis, including metabolic adaptation, regulation of immune evasion, resistance to cell death, tumor cell migration and invasion for tumor promotion; tumor dormancy, and genomic stability maintenance for tumor inhibition (2). On the one hand, in the early stages of cancer, various autophagy-related genes, such as *BECN1* (Beclin 1) and *ATG7* (Autophagy Related 7), which are critical regulators responsible for the initiation stage of autophagy, are involved in tumor inhibition in specific cancer types and specific tissues (2). The loss or mutant of *BECN1* led to the promotion of tumorigenesis in breast, gastric, colon, ovarian, and prostate cancers (3–6). *ATG7* showed a negative correlation with tumorigenesis in pancreatic ductal adenocarcinoma (PDAC), which was not only due to its regulation of autophagy but also its role in invasion and metastasis (7). On the other hand, ALP can contribute to the growth, metabolism, and survival of tumor cells in the later stages by clearing the damaged DNA, proteins, dysfunctional organelles, and toxic oxygen radicals and promoting metastasis (8). In addition, ALP also participates in tumor microenvironment regulation by suppressing immune responses by immune cells (9) and promoting the evasion of immune attacks by degrading the major histocompatibility complex (MHC) Class I (MHC-I) (10). These protective effects of ALP on tumor cells usually lead to the resistance of tumor therapies and poor prognosis.

Transcription factor EB (TFEB) is the primary regulator of autophagy and lysosome biogenesis and an oncogene. Patients with renal cell carcinoma (RCC) (11) and alveolar soft part sarcoma (12) show chromosomal translocations involving TFEB and TFE3 (Transcription Factor Binding To IGHM Enhancer 3) (13). It can be activated under various cellular stresses, such as mitochondrial damage, ER stress, starvation, and pathogen infection (14), which leads to the increasing expression of a wide variety of genes with dual effects on cancer. The dysregulation of TFEB expression and activity are associated with pancreatic cancer cell proliferation (15) and non-small cell lung cancer motility (16). Although the main functions of TFEB in cancers are detrimental through inducing ALP, especially in the later stage of tumor progression, some studies have revealed that TFEB could work as an antitumor factor in an ALP-dependent or independent way. For instance, Liu *et al.* (17) found a TFEB inducer, Tubeimoside-1 (TBM-1), could promote the efficacy of cancer immunotherapy by increasing lysosomal degradation of programmed cell death ligand 1 (PD-L1), which could inhibit the T cell receptor (TCR) pathway. Bellese *et al.* (18) demonstrated that Neratinib (NE) might perform an antitumor effect on breast cancers by increasing and activating TFEB/TFE3 to induce ALP under short-time treatment and to regulate cell cycle arrest, apoptosis, mitochondrial dysfunction, and inhibition of DNA damage response under more extended time treatment. These studies suggest that TFEB might play dual roles in cancer treatments.

TFEB and ALP are usually activated by various cancer-associated risk factors, such as misfolded proteins and damaged organelles, resulting in cell stresses, like reactive oxygen species (ROS) imbalances, inflammation, defective antigen presentation, leading the cells to malignant transformation (2). In addition to the transcript regulation of TFEB, the post-translational regulation of TFEB is more critical for its role in stress response and diseases (19). The activation and nuclear localization of the encoded protein product of *TFEB* are critical for its regulatory function as a transcription factor. The mammalian target of rapamycin (mTOR) pathway-related stress (e.g. nutrition deficiency), mitochondrial damage (e.g. oxidative stress), and lysosomal stress (e.g. lysosome storage) are three common inducers for TFEB activation and promotion of its nuclear localization. Since cancer is one of the stress-related diseases, these stresses are also crucial for the initiation, progression, prognosis and treatment of cancer (20–23). Previous studies on TFEB targets usually focus on a single cellular stress scenario for lysosome or autophagy-related context (24,25). However, the detailed downstream targets of TFEB under different cellular stresses are still poorly studied.

Here, we treated Hela cell lines with three classic TFEB inducers, i.e. carbonyl cyanide *m*-chlorophenylhydrazone (CCCP), sucrose, and Torin1, and confirmed with RNA-sequencing (RNA-seq) and chromatin immunoprecipitation sequencing (ChIP-seq) techniques to explore the regulatory target profiles and multi-functions of TFEB responding to these three stresses. Torin1 is a highly potent and selective ATP-competitive mTOR inhibitor. It can induce autophagy in a mTORC1-dependent and mTORC2-independent way (26). CCCP is a protonophore capable of increasing membrane proton conductance, causing mitochondrial depolarization and uncoupling of respiration. It can lead to PINK1/parkin-mediated mitophagy in an AMPK-independent but mTORC1-dependent manner, activating TFEB (27,28), and it can also induce TFEB nuclear translocation by activating lysosomal TRPML1 (Mucolipin TRP Cation Channel 1) channels, inducing lysosomal Ca^{2+} release (29). As a neutral disaccharide, sucrose was reported to cause a vacuolation model by damaging the osmotic pressure balance between lysosome and cytoplasm, increasing lysosomal gene expression (24). Therefore, to clarify the function of TFEB and decipher genes regulated by TFEB under different stress scenarios, we used these three inducers to induce various kinds of cellular stresses in Hela cell lines and further investigate its regulatory targets through cross-validation by RNA-seq and ChIP-seq. We further constructed a Shinyapp website (https://minglab.shinyapps.io/shiny_pro/) to show this complex regulatory potential of TFEB under different stimuli.

Gene co-expression network analysis has emerged as a powerful tool for predicting gene module functions and identifying disease biomarkers in various cancer types. There have been various methods proposed to construct the networks from high-throughput multi-omics data, such as weighted correlation network analysis (WGCNA) (30) and multiscale embedded gene co-expression network analysis (MEGENA) (31). These approaches provide comprehensive insights into the regulatory mechanisms of cancer development, progression, drug resistance, and patient prognosis (32). Although the gene co-expression network is a comprehensive method to explore the key drivers of essentially biological processes or functions for cancer-related gene modules, there are still some hidden players with indispensable roles in tumor development, progression, and prognosis, which might be a neighbor gene (not the hub gene), or a non-coding gene regulat-

ing the expression of other key driver genes (33–35). From a recent pan-cancer study, we assessed the constructed gene co-expression networks across 32 cancer types from 9 546 individuals in the TCGA database (36). By integrating the pan-cancer gene co-expression networks with our TFEB regulatory profiles, we found that TFEB might work as a hidden player in tumor progression by regulating expressions of risk factors, such as *CXCL2*, *PKMYT1* and *BUB1,* associated with cell cycle and immunosuppression; and by regulating expression of protective factors, such as *CD79A*, related to the activation of T cells and increasing B cell infiltration in the tumor microenvironment (TME). Further studies are needed to validate our findings in different cell lines and further explore the underlying switch between regulating risk factors and protective factors for TFEB. Our findings excavate the potential to regulate cancer progress and influence the prognosis by targeting TFEB or its downstream regulated genes.

Materials and methods

Cell culture and treatment

The cell lines used in this study included Hela cells expressing 3 × Flag-TFEB, Hela cells expressing GFP-TFEB, and Hela wild-type cells. Hela cells expressing 3 × Flag-TFEB were cultured and maintained in DMEM containing 200 μg/ml G418 (Sigma, N1876-25G), 10% fetal bovine serum (FBS, Thermo, #26 140 079-500ml), and 1% Penicillin–Streptomycin (PS, Thermo, 10 378 016–100ml) and cultured in DMEM containing 10% FBS and 1% PS for experiments. Hela wild-type cells and Hela cells expressing GFP-TFEB were cultured in DMEM containing 10% FBS and 1% PS. All cells were maintained in the incubator at 37 °C with 5% CO_2. Hela cell lines were treated with CCCP (20 μM, Med Chem Express, HY-100941) and Torin1 (1 μM, LC Laboratories, T-7887) for 1 h for ChIP-seq and six hours for RNA-seq. Cells were treated with sucrose (150 Mm, Millipore, 573 113) for 6 h for ChIP-seq and eight hours for RNA-seq. The figures for HeLa cells expressing GFP-TFEB were taken using the Opera Phenix Plus High-Content Screening System (PerkinElmer).

RNA-sequencing and differential gene expression analysis

For RNA-seq, cells were seeded in one 6cm dish/group and were cultured to around 80% confluent, followed by corresponding treatment. After treatment with vehicle, CCCP, sucrose and Torin1, followed by washing with PBS (phosphate buffer saline, Thermo, #21 600 010), cell samples were collected and maintained using RNA stabilization and storage solution (RNA*later*™, Thermo, AM7020). Then, the RNA extraction followed by reversing transcription with an oligo-dT primer, RNA library preparation, and paired-end sequencing were performed at the DNBSeq platform by Bioyi Biotechnology Co., Ltd Wuhan. Three biological repeats were performed in each group. After being filtered by Fastp (37) and qualified by FastQC (https://qubeshub.org/resources/fastqc), reads were aligned to the hg38 RefSeq database using HISAT2 (38). The gene count matrix and transcript count matrix were generated by Stringtie (39). Genes with FPKM (fragments per kilobase per million mapped reads) larger than or equal to 0.1 were included. Principal component analysis (PCA) was performed based on the normalized gene count matrix, and the PCA plot was generated by R using the ggplot2 package (40). Differential gene expression analysis was performed using DESeq2 (41). Differential expression genes (DEGs) were selected based on corrected p-value using the Benjamini-Hochberg method (P_{adj}) <0.05 and fold change (FC) > 1.5 or < –1.5. The Venn diagrams were generated by an R package, VennDiagram (42). Gene ontology (GO) and pathway enrichments were performed using Metascape (43). The boxplots of genes are displayed on the shiny app website (https://minglab.shinyapps.io/shiny_pro/) constructed using shiny (https://shiny.posit.co/). The Dunnett's multiple comparison test was performed after analysis of variance (ANOVA) for the comparisons between two groups.

ChIP-sequencing

For ChIP assays, Hela cells with or without expressions of 3 × Flag-TFEB after treatments with or without CCCP, sucrose, and Torin1, followed by washing with PBS, were fixed with formaldehyde (Sigma, F8775-500ml) to a final concentration of 1% (v/v) for 10 mins at room temperature (RT) with gentle shaking. Afterward, stop the cross-linking reaction by adding glycine (Sigma, G8898-500g) to a final concentration of 0.125 M and continue shaking for 5 min. Then, after washing with pre-cooling PBS three times, cells were collected for nuclei preparation and chromatin shearing using the ChIP Kit from ZYMO Research (D5209) according to its manual with gentle adjustments. We sheared the chromatins by sonicating them on ice for 6 × 5 cycles (30 s 'ON', 30 s 'OFF' at 40% amplitude) to make sure that the chromatin DNA fragments were 100–500 bp average in size. An equal quantity of DNA fragments in each group was immunoprecipitated with 50μl Anti-FLAG® M2 Magnetic Beads (Sigma, M8823) overnight at 4°C with 1% of the diluted complex as input groups. The tubes were placed on a magnetic stand the next day, and the supernatants were discarded. After washing and eluting the beads according to the kit manual, the protein-DNA complex was reversed by heating at 65°C overnight. According to the manual, immunoprecipitated DNA was purified by the kit and subjected to library construction and high throughput sequencing by the Beijing Genomics Institution (BGI).

ChIP-seq data processing and analysis

Clean sequencing reads were aligned to the hg38 RefSeq database using Bowtie (44) and then were qualified by FastQC. After removing the reads that duplicated as the artificial product of the PCR step of library preparation, peaks were determined by MACS2 (Model-based analysis of ChIP-seq 2) (45) using input DNA as the negative control and the default parameters with minor modifications (i.e. '–extsize 200', '–p 0.01'). We merged the qualified reads of two replicates for further study because more than 40% of the identified pull-down peaks by TFEB in the second replicate were shared with the first replicate. Then, the peaks were annotated using the default parameters by HOMOR (Hypergeometric Optimization of Motif Enrichment) (46). The promoter peaks were defined as those localizing from 1000 bp downstream to 5000 bp upstream of transcript start sites (TSS). Genes with TFEB binding sites in the promoter region were included for further study. We performed a ngsplot program (47) to investigate the enrichment of TFEB by targeting peaks of genes in the gene body.

Hypergeometric test

In the previous study (36), there were 27 448 pan-cancer modules across 32 cancer types including hub genes and neighbor genes, which were constructed based on the gene co-expression networks using MEGENA. After the calculation of correlation (*false-discovery rate, FDR* < 0.05), construction of planar filtered networks (PFNs), and multi-scale clustering analysis (MCA), the pan-cancer modules were identified and then structured in a hierarchy. The nodes with significantly ($P < 0.05$) higher network connectivity than the randomly permuted planar networks were identified as the hub genes according to the multiscale hub analysis and other nodes in the modules were identified as neighbor genes (31). These pan-cancer modules were categorized into conserved and specific modules according to the Fisher Exact test (FET) and the Jaccard similarity index (JSI) for the module similarity among all cancer types. 1 941 conserved modules (7% of total network modules with $JSI > 0.4$) showed significant similarities in molecular regulatory patterns of cancer transcriptomes in all 32 included cancer types, while 1 063 specific modules (4% of total network modules with $JSI < 0.05$ or $FET.P > 0.05$) showed their specificality in particular cancer types. We recognized the intersections between the genes in pan-cancer modules (hub genes or neighbor genes) and our identified TFEB targets through hypergeometric tests, accomplished by the R function phyper, and the p-value was corrected using the Benjamini-Hochberg method. After adjustment, those with an adjusted p-value (P_{adj}) < 0.05 were defined as significant enrichments.

Survival analysis and gene expression

The expression levels of genes among normal tissues and tumor tissues and survival rate data for cancers were collected from the Cancer Genome Atlas (TCGA) project using GEPIA (Gene Expression Profiling Interactive Analysis, http://gepia.cancer-pku.cn/). In GEPIA, the high-expression and low-expression groups were classified depending on the median of the expression levels of genes. The gene expression levels in tumor stages were collected by the University of Alabama at Birmingham Cancer Data Analysis Portal (UALCAN) (48). The significance of the differences in mRNA expression levels between normal and tumors was estimated using Welch's t-test. The protein levels of TFEB and phosphorylated TFEB at Ser142 were collected from the Clinical Proteomic Tumor Analysis Consortium (CPTAC) (49) through UALCAN. The significance of the differences in protein or phosphorylated protein expression levels between normal and tumors was estimated using the t-test.

Results

Transcriptomic and epigenetic changes induced by TFEB are consistent in regulating cancer pathways responding to different stresses

Since the activated TFEB can translocate into nuclei, to investigate the downstream regulation of this shift of TFEB between nuclei and cytoplasm more efficiently, we used Hela cells expressing 3 × Flag-TFEB in the experiments of RNA-seq and ChIP-seq. We first treated Hela cells expressing 3 × Flag-TFEB with or without three TFEB inducers (i.e. CCCP, sucrose, and Torin1). Then, we detected the TFEB potential target genes using RNA-seq by comparing them with non-treated (i.e. Ctrl) cells. We expressed GFP-TFEB in Hela cells and they showed apparent GFP-TFEB nuclear translocation after treatment with these three inducers (Figure 1A). RNA-seq showed that the gene expression patterns were heterogeneous among groups (Figure 1B). We identified 5754 significantly upregulated DEGs ($FC > 1.5$ and $P_{adj} < 0.05$) compared with the Ctrl group in total under three inducers (Figure 2A). These DEGs can be divided into five groups: CCCP-specific, Sucrose-specific, Torin1-specific, Two stimuli-overlapped, and Three stimuli-overlapped DEGs (Figure 2A, Supplementary Table S1). The function enrichment analysis showed that in addition to pathways in cancer (KEGG: hsa05200), these five groups containing TFEB potential targets took part in cell division, cellular response to stimuli (i.e. lipid, cytokine stimulus, hormone, starvation, etc.), regulation of secretion, regulation of the immune system (e.g. cytokine signaling in immune system and cell activation), and positive regulation of locomotion (Figure 2B).

To avoid off-target bias from RNA-seq, we further confirmed the genes whose expressions were directly regulated by activated TFEB under the same three different cellular stresses through ChIP-seq for the DNA fragments pulled down by TFEB using Hela cells expressing 3 × Flag-TFEB (Figure 1C). Most DNA fragments were enriched near transcription start site (TSS) regions (Figure 1D). We identified 10 824 genes with TFEB binding sites in the promoter region under three stimuli (Figure 2C) and categorized them into five groups, the same as DEGs (Supplementary Table S1). In line with those significantly upregulated DEGs, these genes were enriched in functions related to cancer progression and prognosis, e.g. pathways in cancer (KEGG: hsa05200), regulation of DNA metabolic process, cell cycle, viral infection, DNA damage response, transcriptional regulation by TP53 and so forth (Figure 2D). Notably, some genes were identified as TFEB targets by ChIP-seq but were not upregulated DEGs, revealing that the expressions of these TFEB targets might not be stress-dependent, such as *BECN1* and *ATG7* (Figure 6K, L). TFEB binding alone might not be sufficient for these gene activations. Other co-factors or additional signals might be required for full transcriptional activation of these genes.

To further determine that TFEB directly regulated the mRNA expressions of these genes responding to these three stimuli, we integrated the genes identified by both RNA-seq and ChIP-seq and obtained 2182 confirmed TFEB targets (Figure 2E, Supplementary Table S1). Except for the TFEB classical functions related to autophagy, lysosome, and cellular response to amino acids starvation, these targets also play essential roles in cancer progress and prognosis, such as regulation of apoptotic signal pathway and programmed cell death, adipogenesis, and circadian clock (Figure 2F). These results indicate that TFEB might play multiple roles in cancer through transcriptomic and epigenetic regulations when responding to various stresses.

Furthermore, to investigate whether there are novel TFEB targets responding to stress, we accessed two different databases for TFEB targets from reported studies or published experimental data, i.e. Gene Set Enrichment Analysis (GSEA) (50) and ChIP Enrichment Analysis (ChEA) (51), including 1417 and 799 TFEB targets respectively. 24.5% of the reported TFEB targets were identified in our study, proving the reliability of our research. In total, 1712 genes might be novel TFEB targets responding to one or more stimuli according to the integration of transcriptomic and epigenetic data

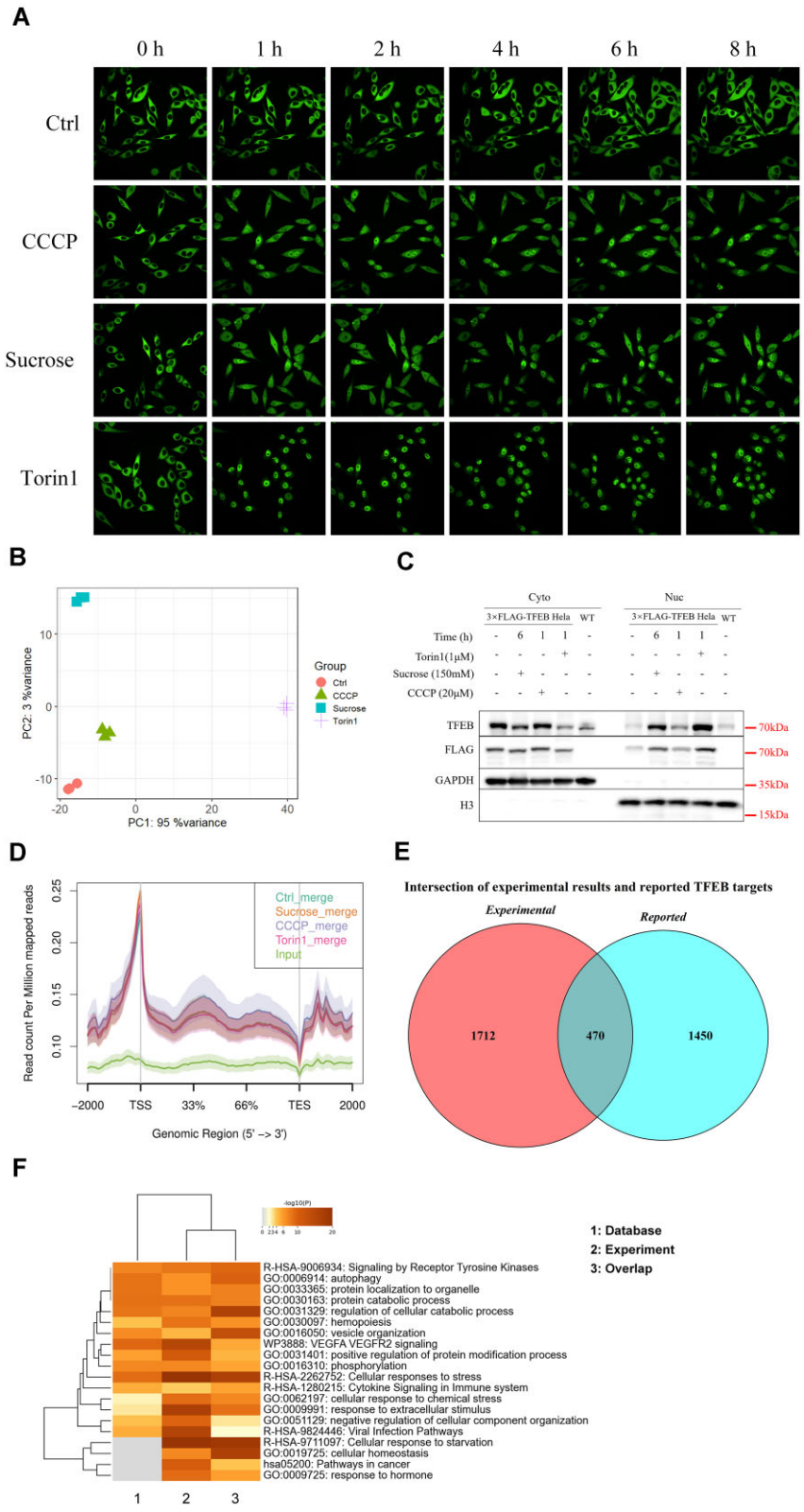

Figure 1. TFEB showed nuclear translocation under three different stresses. (**A**) GFP-TFEB translocated into the nucleus in Hela cells expressing GFP-TFEB under three different treatments; (**B**) PCA plot for RNA-seq expression matrix; (**C**) Nuclear translocation induced by CCCP (20 μM, 1 h), sucrose (150 mM, 6 h) and Torin1 (1 μM, 1 h). (**D**) Average profiles of peak enrichment in the whole gene body regions of genes identified by ChIP-seq under three stimuli; (**E**) Intersection of reported and unreported TFEB targets; (**F**) Function enrichment of TFEB targets in (E).

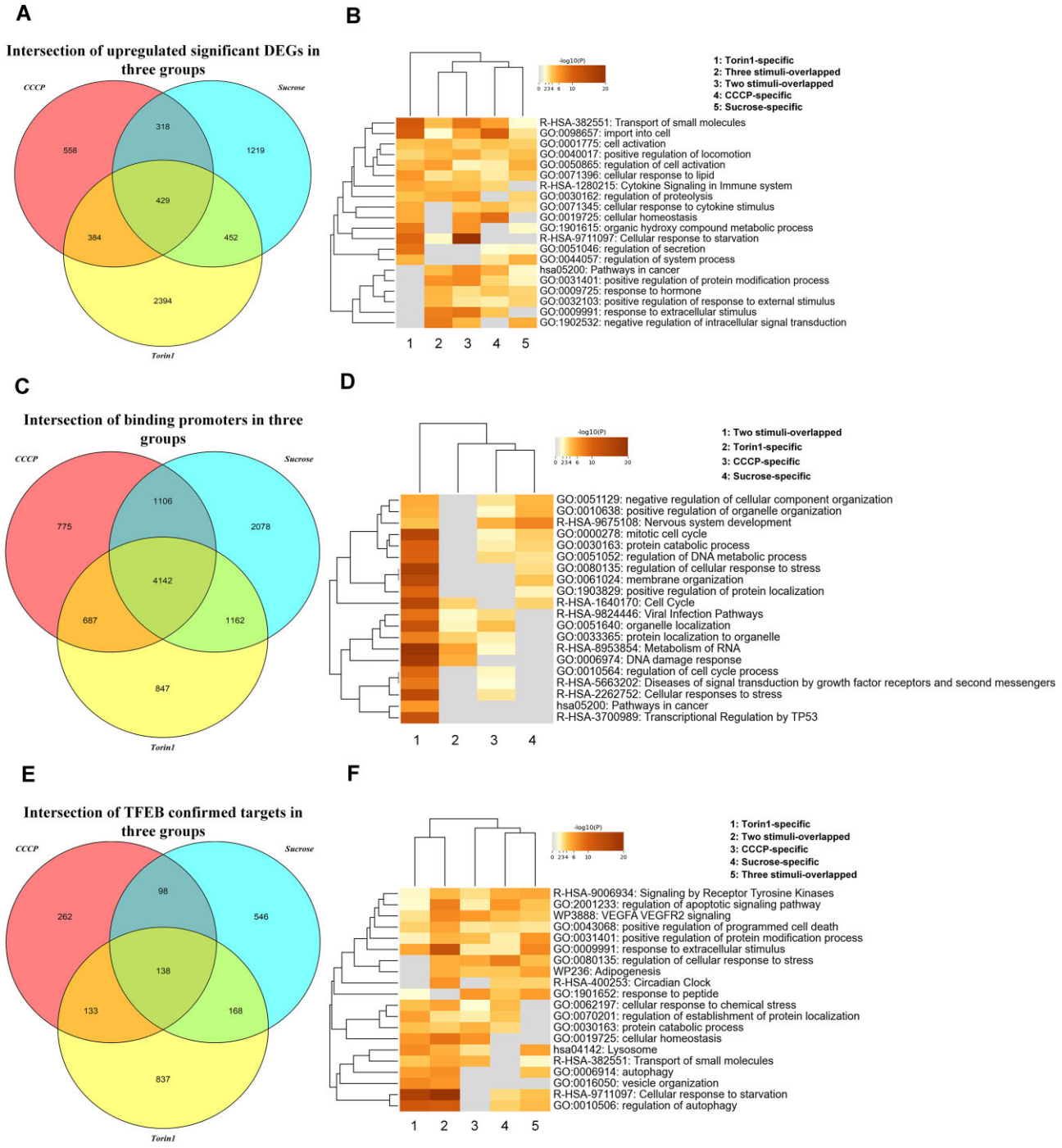

Figure 2. TFEB regulates various pathways. (**A**) Overlap of upregulated DEGs ($FC > 1.5$, $P_{adj} < 0.05$) under three stimuli; (**B**) function enrichment of five groups of upregulated DEGs (i.e. CCCP-specific, sucrose-specific, Torin1-specific, two stimuli-overlapped, and three stimuli-overlapped); (**C**) The identified promoters under three stimuli; (**D**) Function enrichment of four groups of upregulated identified promoters; (**E**) Overlap of confirmed TFEB targets in transcriptomic and epigenetic levels; (**F**) Function enrichment of five groups of confirmed TFEB targets.

(Figure 1E). In addition to previously known functions associated with ALP, metabolic process, and cellular responses to stress (e.g. starvation), these novel TFEB targets also showed enrichment in pathways in cancer (KEGG: hsa05200), hemopoiesis, viral infection pathways, response to extracellular stimulus, negative regulation of cellular component organization, etc. (Figure 1F). Our study identified 1 712 novel TFEB targets and suggested that TFEB and its targets were involved in multiple cancer-related pathways.

The confirmed TFEB targets are distributed among the co-expression network of Pan-cancer

To further explore the roles of TFEB and its targets in cancer, we next adopted the gene co-expression networks from a recent pan-cancer study (36), in which the constructed co-expression networks by MEGENA covered 32 cancer types from 9546 individuals in the TCGA database and included 19 757 genes from 27 448 modules. We compared the MEGENA networks with our TFEB targets and found that

the identified 2182 confirmed TFEB targets were distributed among 4517 modules among 32 cancers (Supplementary Figure S1). The confirmed TFEB targets in CCCP-specific, Torin1-specific, two stimuli-overlapped, and three stimuli-overlapped groups were significantly enriched ($P_{adj} < 0.05$) in 84 modules for 24 cancers (Figure 3A, Supplementary Table S2). These modules showed enrichment in similar functions associated with metabolic process, translation, covalent chromatin modification and protein folding, skeletal muscle cell differentiation, regulation of peptidyl tyrosine phosphorylation, oxidative phosphorylation, transmembrane transport, mitochondrial organization, etc. (Supplementary Figure S2). In addition to autophagy lysosomal pathways and metabolic processes, the confirmed TFEB targets in these four groups were enriched in the immune system process, developmental process, detoxification, etc. (Figure 3C).

Notably, the confirmed three stimuli-overlapped TFEB targets were significantly enriched in 18 modules from nine cancers with 40 genes (Figure 3B, Supplementary Table S2) ($P_{adj} < 0.05$). Within these modules, STAD_M222 for stomach adenocarcinoma (STAD), including 17 significant down-regulated cancer DEGs ($P_{adj} < 0.05$), showed a high hazard ratio ($HR = 1.54$, $P = 0.014$) (Figure 3D), while most of the DEGs were down-regulated ($P_{adj} < 0.05$). Eight of 17 were TFEB targets enriched in the AP-1 pathway, ATF2 pathway, and corticotropin-releasing hormone signaling pathway. UCEC_M435 for uterine corpus endometrial carcinoma (UCEC), including 17 significant upregulated cancer DEGs, also showed a high hazard ratio ($HR = 1.61$, $P = 0.034$), and most of the DEGs were upregulated ($P_{adj} < 0.05$) (Figure 3E). Two TFEB targets, *GDF15* and *FOSL1*, significantly upregulated in this module, were mainly involved in the ERBB2-EGFR signaling pathway. It indicates that the significant DEGs in the STAD_M222 module might protect against cancer, while those in the UCEC_M435 module might harm and promote tumorigenesis. These results suggest that TFEB targets are widely distributed in the co-expression networks among cancers involved in regulating cancers as risk factors or protective factors under different stresses.

TFEB upregulates hub gene expressions of Pan-cancer co-expression network modules

Interestingly, despite being one of the oncogenes, TFEB was not a hub gene among all the identified modules in pan-cancer co-expression networks. However, its targets were widely distributed among the Pan-cancer modules. According to the Fisher Exact test and the Jaccard index of module similarity for pairwise module comparisons of all cancer types, the pan-cancer modules were categorized into conserved and specific modules (Materials and method). 1 941 conserved modules showed significant similarities in molecular regulatory patterns of cancer transcriptomes in all 32 included cancer types, while 1 063 specific modules showed their specificality in particular cancer types (36). We performed the hypergeometric tests between the hub genes of these 3 004 pan-cancer modules and upregulated DEGs induced by activated TFEB in five groups (Supplementary Table S3, Method). TFEB-induced DEGs in all five groups are significantly enriched in the hub genes of conserved Pan-cancer modules among 32 cancer types ($P_{adj} < 0.05$) (Figure 4A). The functions of these hub genes showed strong associations with cancer, such as the biological process for immune response, regulation of cellular stress response, and regulation of ubiquitin (Figure 4B).

In addition, DEGs in the Torin1 group were significantly enriched in the hub genes of five modules for specific cancers, i.e. adrenocortical carcinoma (ACC), lymphoid neoplasm diffuses large B-cell lymphoma (DLBC), testicular germ cell tumors (TGCT), thymoma (THYM) and uveal melanoma (UVM) ($P_{adj} < 0.05$). These hub genes in the five cancer types had different functions (Figure 4C). Most DEGs were enriched in THYM, mainly associated with epithelial cell migration. In TGCT, the enriched hub genes were involved in osteoblast differentiation. In UVM, the enriched hub genes regulated cellular response to grow factor stimulus and chordate embryonic development. According to the ChIP-seq data, these DEGs were directly bound with TFEB around the promoter regions (Supplementary Figure S3A–E).

There were more TFEB potential targets identified by ChIP-seq significantly enriched in the pan-cancer co-expression network modules ($n = 24$, $P_{adj} < 0.05$) (Supplementary Figure S3F). The potential TFEB targets involved in the hub genes of cancer modules showed similar function enrichment to those mentioned above, especially some important for cancer progression, such as DNA replication, T cell activation, stress response to metal ion, response to cAMP, etc. These results indicated that TFEB might had hidden roles in cancer progression by regulating the expression of hub genes of essential modules in the co-expression networks in cancers.

The confirmed TFEB targets work as key drivers in pan-cancer co-expression networks

We further confirmed the regulatory functions of TFEB in pan-cancer by combining the transcriptomic and epigenetic results. Hypergeometric tests showed that 111 TFEB potential targets in four groups (i.e. CCCP-specific, sucrose-specific, Torin1-specific, and two-group overlap) were significantly enriched with the hub genes of conserved Pan-cancer modules ($P_{adj} < 0.05$). Besides, other five confirmed TFEB targets were induced by three stimuli, i.e. *FOSB* (FosB Proto-Oncogene, AP-1 Transcription Factor Subunit), *NR4A1* (Nuclear Receptor Subfamily 4 Group A Member 1), *MORC3* (MORC Family CW-Type Zinc Finger 3), *INSIG1* (Insulin Induced Gene 1) and *THFAIP3* (TNF Alpha Induced Protein 3), were hub genes of conserved Pan-cancer modules (Figure 4D, Supplementary Table S4). In total, 116 confirmed TFEB targets, enriched in similar functions and pathways as mentioned above, were hub genes among 1451 conserved pan-cancer modules of 32 cancers. Some of these confirmed TFEB targets had protein-protein interactions (PPI) with others (Figure 4F). The function enrichment analysis highlighted their roles in not only the regulation of TORC1 signaling but also cell cycle, immune system process, viral process, response to stimuli, metabolic process, etc., which are all important for cancer treatment and prognosis (Figure 4E).

In addition, among the referred conserved modules, 183 modules had a significant hazard ratio ($P < 0.05$) with genes enriched in functions related to the immune system, such as T cell activation, B cell activation, neutrophil migration, and defense response to virus; mitotic cell cycle, such as mitotic nuclear division, organelle fission, and chromosome segregation; metabolic process, such as cellular amino acid metabolic process, ncRNA metabolic process, sulfur compound catabolic process, DNA replication, etc.; ATP synthesis

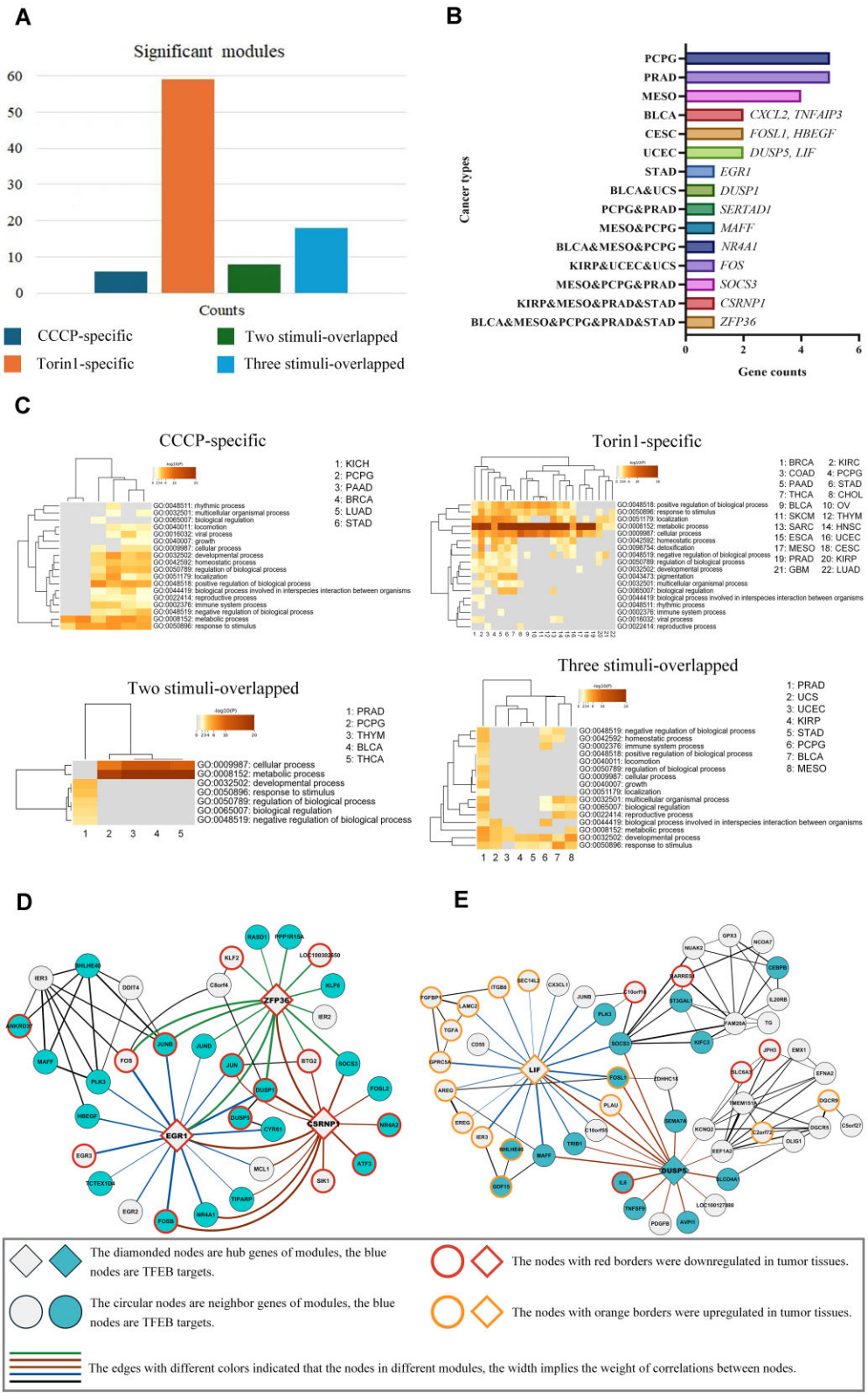

Figure 3. The distribution of confirmed TFEB targets among all Pan-cancer modules. (**A**) Numbers of Pan-cancer modules among five groups of confirmed TFEB targets; (**B**) The confirmed TFEB targets in three-group overlap were distributed in 18 modules of 9 cancers; PCPG: pheochromocytoma and paraganglioma; PRAD: prostate adenocarcinoma; MESO: mesothelioma; BLCA: bladder urothelial carcinoma; CESC: cervical squamous cell carcinoma and endocervical adenocarcinoma; UCEC: uterine corpus endometrial carcinoma; STAD: stomach adenocarcinoma; UCS: uterine carcinosarcoma; KIRP: kidney renal papillary cell carcinoma. (**C**) Function enrichment of the confirmed TFEB targets included in the pan-cancer modules. (**D**) The sub-network of STAD_M222 module; (**E**) The sub-network of UCEC_M435 module.

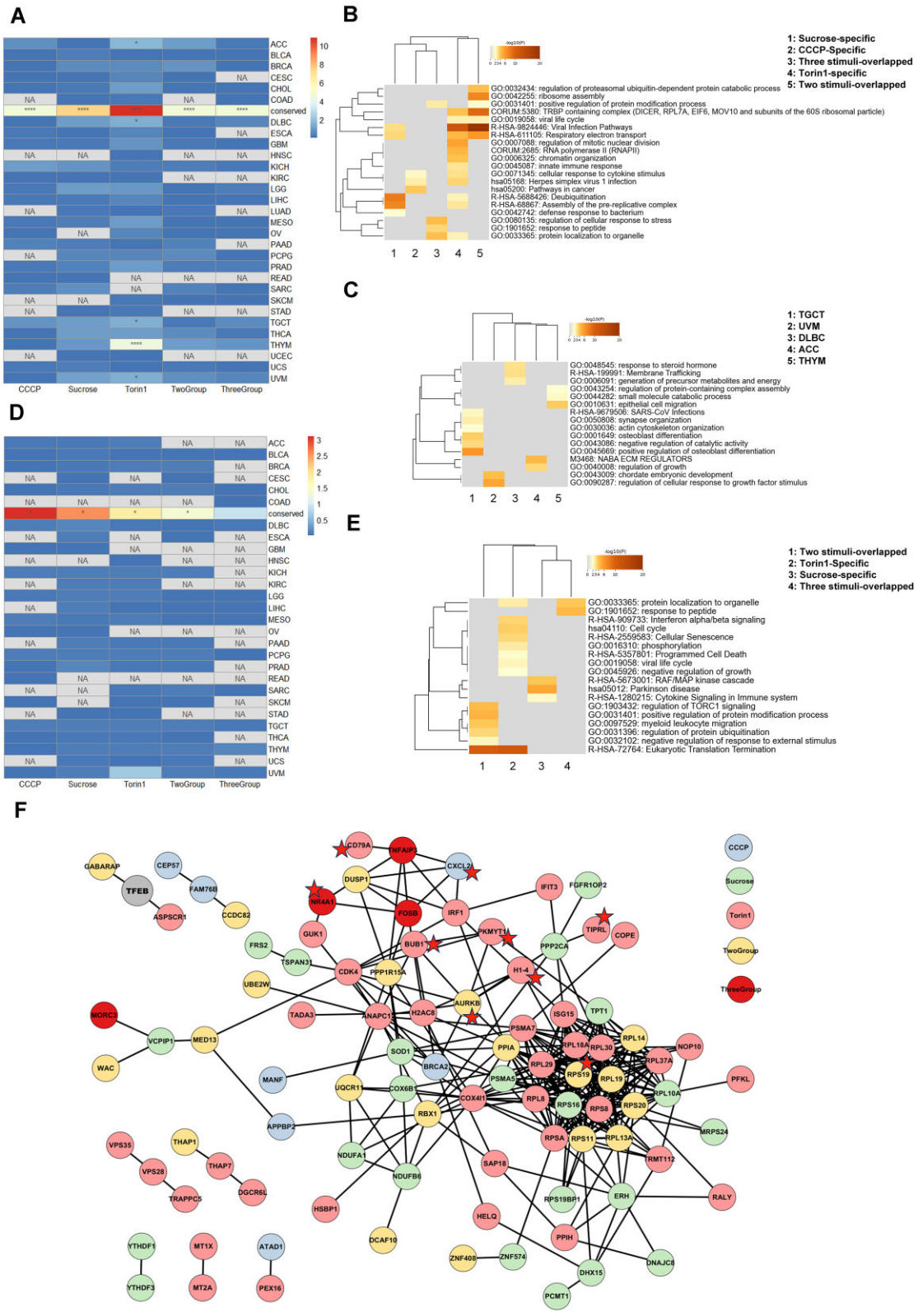

Figure 4. Enrichment of TFEB targets in hub genes of pan-cancer co-expression networks. (**A**) Heatmap of hypergeometric tests results among upregulated DEGs by TFEB and hub genes of Pan-Cancer co-expression network; (**B**) Function enrichment of significant genes by the hypergeometric tests among five experimental groups and conserved Pan-cancer modules; (**C**) Function enrichment of significant genes by the hypergeometric tests among Torin1 group and five cancer-type-specific modules; (**D**) Heatmap of results of hypergeometric tests among confirmed TFEB targets and hub genes of Pan-Cancer co-expression network; (**E**) Function enrichment of confirmed TFEB targets among five groups significantly enriched in conserved Pan-cancer modules; (**F**) The protein–protein interactions (PPI) of 116 confirmed TFEB targets significantly enriched in the hub genes of conserved Pan-cancer modules. The stars marked the genes with significant survival results in cancers. $*P < 0.05$, $**P < 0.01$, $***P < 0.001$, $****P < 0.0001$.

coupled electron transport; translation and protein location (Supplementary Figure S4). Therefore, the confirmed TFEB targets enriched in multi-functions might play crucial roles in the cancer progression and prognosis by regulating the genes in conserved modules of pan-cancer.

TFEB targets play dual functions in pan-cancer

To further define whether the confirmed TFEB targets work as protective or risk factors for tumorigenesis and prognosis in pan-cancer, we employed the below criteria to define protective or risk factors: (i) it is the hub gene of crucial modules in pan-cancer networks; (ii) it shows a significant survival rate in cancers; (iii) it is differentially expressed gene in tumor tissues compared to the normal tissues; (iv) it or its regulated modules are enriched in cancer-related functions or pathways (Materials and methods). If the hazard ratio (HR) calculated by survival analysis is larger than 1, the TFEB target is considered as a cancer risk factor. If the HR is smaller than 1, the TFEB target is considered an anti-cancer protective factor. It is a comprehensive screening strategy to find promising targets for therapy against cancer.

First, we compared their expression levels between tumor tissues and normal tissues in 17 cancers included in TCGA databases (Materials and method). 32 of 116 confirmed TFEB targets, which were hub genes of 155 conserved modules, were significant DEGs in 16 cancers ($\log FC > 1$ or < -1, $P_{adj} < 0.05$). These upregulated DEGs in tumor tissues worked as hub genes of modules mainly enriched in functions associated with organelle fission, chromosome segregation and cotranslational protein targeting to membrane, and most of these modules indicated poor prognosis ($HR > 1$, $P < 0.05$). The downregulated DEGs in tumor tissues worked as hub genes of modules mainly enriched in functions associated with extracellular structure organization, response to molecule of bacterial origin, and T cell activation, and these modules indicated better or poor prognosis depending on different cancer types (Supplementary Table S5).

Next, we performed the survival tests for the 32 confirmed TFEB targets (Materials and method). Nine genes, i.e. *AURKB* (Aurora kinase B), *BUB1* (BUB1 mitotic checkpoint serine/threonine kinase), *PKMYT1* (Protein kinase, membrane-associated tyrosine/threonine 1), *CXCL2* (C-X-C motif chemokine ligand 2), *NR4A1*, *RPS19* (ribosomal protein S19), *TIPRL* (TOR Signaling Pathway Regulator), *HIST1H1E/H1-4* (H1.4 Linker Histone, Cluster Member), and *CD79A* (CD79a Molecule), had significant survival rates ($P < 0.05$) (Figures 4F and 5A). They were mainly enriched in functions related to the negative regulation of cell cycle and cell chemotaxis (Figure 5B).

AURKB, *BUB1* and *PKMYT1* play critical roles in DNA-dependent DNA replication and mitosis, especially chromosomal segmentation and organelle fission. They all expressed higher in tumor tissues than normal tissues with poor survival rates ($P < 0.05$). *AURKB* was upregulated by CCCP and Torin1 (Figure 6A). The higher expressions of *AURKB* showed poor prognosis in KIRC, kidney renal papillary cell carcinoma (KIRP), and lung adenocarcinoma (LUAD) (Figure 5C). *BUB1* and *PKMYT1* were targeted by TFEB with Torin1 treatment (Figure 6B,C). The higher expressions of *PKMYT1* showed poor prognosis in KIRC, KIRP, liver hepatocellular carcinoma (LIHC) and LUAD (Figure 5D), and the higher expression of *BUB1* showed a lower survival rate in LUAD (Figure 5E). These three TFEB targets might be risk factors for the corresponding cancers.

Three other TFEB targets, *CXCL2*, *NR4A1* and *RPS19*, which differentially expressed and had a significant effect on the prognosis in lung squamous cell carcinoma (LUSC), thyroid carcinoma (THCA) and KIRP respectively (Figure 5F–H), mainly involved in cell chemotaxis. *CXCL2* was strongly targeted by TFEB in the CCCP-specific group (Figure 6D) and expressed lower in tumor tissues than normal tissues in LUSC (Figure 5F). However, the high expression of *CXCL2* showed a poor survival rate ($P < 0.05$) (Figure 5F). *NR4A1* was upregulated by TFEB under three stimuli (Figure 6E) and expressed lower in tumor tissues, while with a lower survival rate in the high expression group in THCA. *RPS19* was included in the two-group overlap group and upregulated by TFEB, especially with sucrose treatment (Figure 6F). It was expressed more in tumor tissues with a poor survival rate. Therefore, *CXCL2* might work as a risk factor in LUSC, *NR4A1* might be a risk factor in THCA, and *RPS19* might be a risk factor in KIRP.

TIPRL and *HIST1H1E/H1-4* (Figure 6G,H) were involved in the negative regulation of the cell cycle in kidney chromophobe (KICH) and colon adenocarcinoma (COAD) (Figure 5I,J). Although they did not express differentially in the corresponding cancers, *TIPRL* showed lower expressions with a better survival rate ($P < 0.05$). In comparison, *HIST1H1E* showed higher expressions accompanied by a poor survival rate ($P < 0.05$) (Figure 5I, J). The pan-cancer modules for KICH with hub gene *TIPRL* were mainly associated with the cellular amino acid metabolic process and the uranic acid metabolic process. The pan-cancer modules for COAD with *HIST1H1E* as one of the hub genes showed higher HR ($P < 0.05$) associated with chromatin assembly. These results indicated that *TIPRL* might be a risk factor in KICH, and *HIST1H1E* might be a risk factor in COAD.

Notably, *CD79A*, targeted by TFEB under Torin1 treatment (Figure 6I), encodes the protein Igα in cooperation with CD79B (Igβ), making up the B-cell antigen receptor (BCR) complex responsible for the B-cell development and function (52). Furthermore, it worked as a driver gene in modules enriched with B cell activation, T cell activation, leukocyte migration, and cytosolic calcium ion transport in KIRP. The higher expression of *CD79A* showed better survival rates in both LIHC and LUAD (Figure 5K). It showed no significant differences in expression between tumor tissues and normal tissues in LIHC. Although it was expressed higher at the early stages in tumor tissues of LUAD, the expression level decreased at later stages (Supplementary Figure S5). It revealed that *CD79A* might be a protective factor in LIHC and LUAD.

Furthermore, we found that TFEB total protein levels were higher in tumor tissues of clear cell renal cell carcinoma and LUAD with more phosphorylated TFEB at S142 (NP_001161299.2: S437) for the former cancer type while less for the later one according to the proteomic data from Clinical Proteomic Tumor Analysis Consortium (CPTAC) database (Supplementary Figure S6A,B). TFEB protein levels were lower in tumor tissues of LUSC with less phosphorylated at S142 (Supplementary Figure S6C). Phosphorylated TFEB at S142 is usually one of the inactivated forms of TFEB. Hence, the lower levels of phosphorylated TFEB at S142 in tumor tissues of LUAD and LUSC might contribute to the increased mRNA expression of *AURKB*, *BUB1*, *PKMYT1*, *CXCL2* and *CD79A*.

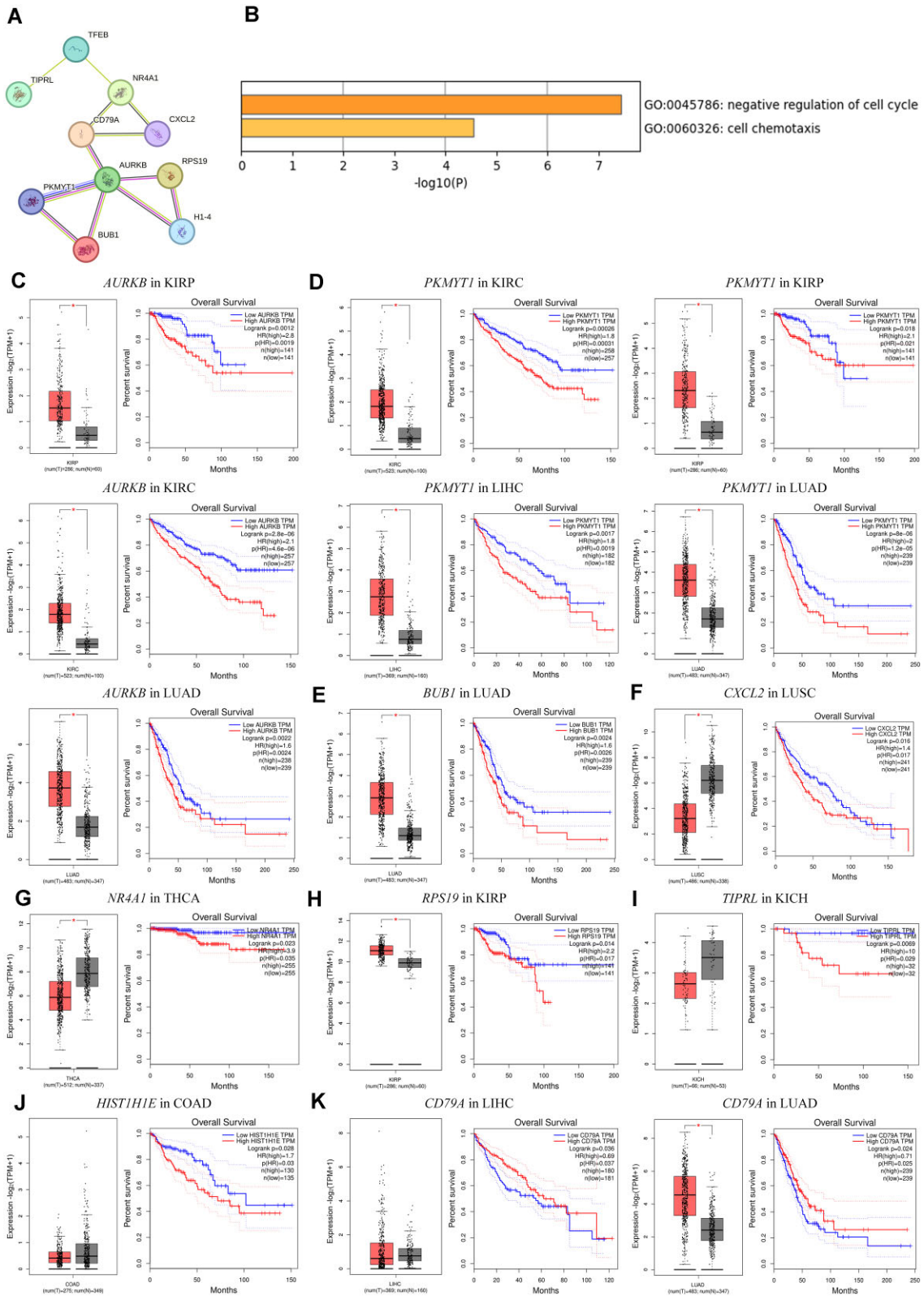

Figure 5. Dual roles of TFEB confirmed targets in pan-cancer. (**A**) PPI network of confirmed TFEB targets; (**B**) Function enrichment of nine confirmed TFEB targets; (**C–K**) Expression levels and survival curve of TFEB targets in different cancers. T means tumor tissue, and N means normal tissue. Plots were drawn by using GEPIA. $*P < 0.05$, $**P < 0.01$, $***P < 0.001$, $****P < 0.0001$.

In summary, TFEB targets play dual functions in pan-cancer. The targets associated with the biological processes, such as mitosis, regulation of the cell cycle, and cell chemotaxis might be risk factors for poor prognosis of cancers. The targets contributing to the immune system are more likely to be protective factors but might change during the different cancer stages.

Discussion

As the primary regulator of the autophagy-lysosomal pathway, the various roles of TFEB in human cancer were well reported (53). However, a systematic investigation of the dichotomous effects of TFEB and downstream targets regulating pan-cancer progression and prognosis has been missing. This study integrated the transcriptomic and epigenetic regulation of TFEB responding to stresses to discover many reported and 1712 novel potential TFEB targets. It provided references for the TFEB downstream targets responding to three stresses and a comprehensive analysis of the potential to regulate pan-cancer progress and influence the prognosis by targeting TFEB or its downstream regulated genes. We found that TFEB was not the hub gene of any modules included, but it could upregulate the expression of various targets under different stresses. 116 TFEB targets were hub genes of conserved Pan-cancer modules. 111 of 116 genes were not reported in the Gene Set Enrichment Analysis (GSEA) and ChIP Enrichment Analysis (ChEA) databases. TFEB might work as a hidden player with dichotomous roles by regulating expressions of risk factors, such as *CXCL2*, *PKMYT1* and *BUB1,* to escape cell cycle arrest and immunosuppression, and protective factors, such as *CD79A,* to activate the anti-tumor TME. Therefore, targeting TFEB downstream targets for cancer therapy is promising due to their multiple functions.

Previous studies have reported various TFEB downstream targets. Overexpressing TFEB can also induce the expression of some TFEB targets, such as *BECN1*, *SQSTM1*, *ATG7*, etc. However, since many stresses are critical for cancers, such as mitochondrial stress (54–56), lysosomal stress (57), and mTOR inhibition (58,59), to focus on regulating TFEB which responds to different stress scenarios, we determined the up-regulated DEGs directly regulated by TFEB responding to CCCP, sucrose, and Torin1 through RNA-seq and ChIP-seq. In addition to the common functions across three treatment groups, such as autophagy, lysosome, cellular response to cellular stress, et al., there were also enriched functions apt to specific treatment groups, e.g. response to endoplasmic reticulum stress and unfolded protein response (UPR) in the CCCP group; regulation of growth, regulation of lipid metabolic process, positive regulation of locomotion in the sucrose group; cellular response to starvation, neutrophil degranulation, congenital generalized lipodystrophy, et al., in Torin1 group. It implies that activated TFEB mainly regulates the expressions of genes related to ALP in normal conditions and those in various downstream pathways under different stresses.

According to our results, except for ALP, TFEB targets induced by these three stimuli participated in the joint and specific biological processes or pathways associated with cancer, such as angiogenesis, apoptosis process, circadian clock, response to peptide, cell-to-cell communication, adaptive immune system, DNA damage response and so forth. Importantly, we revealed that TFEB targets in cancers might work as protective factors against cancer or risk factors for increasing death or poor prognosis. Accordingly, we found some valuable candidates, which might be protective factors to anti-cancer or risk factors to promote cancer. For instance, as a potential novel TFEB target, *CD79A* showed better survival rates in both LIHC and LUAD with higher expressions, although studies reported that it was associated with poor prognosis in DLBC due to promoting the proliferation and survival of malignant B cells (60). Besides, *CD79A* can work as a signal transduction molecule, activating downstream signal pathways to promote chimeric antigen receptor (CAR) T cells, increasing anti-tumor efficacy (61). Since the expression of *CD79A* is related to the infiltration of B cells in the TME, the potential protective effects of *CD79A* from our results might be due to its ability to promote B cell infiltration, which was accompanied by better prognosis according to the analysis of the single-cell RNA sequencing (scRNA-seq) datasets in hepatocellular carcinoma (HCC) tumor samples (62). Thus, *CD79A* might be a risk factor in promoting the proliferation and survival of malignant B cells but a protective factor in the activation of T cells and increasing B cell infiltration in TME.

Notably, in addition to *CD79A*, some risk factors, i.e. *AURKB*, *BUB1*, *PKMYT1* and *TIPRL* are all novel identified TFEB targets in our study, validated by ChIP-seq. They are involved in the regulation of the cell cycle (63–65) and mTOR signaling pathway (66,67) which are important for tumor cell growth and death. They were reported as potential pharmacological and genetic therapy targets (67–72). Furthermore, *CXCL2* was reported in the GSEA database as a TFEB target gene, supporting our RNA-seq and ChIP-seq results. It is an important proinflammatory mediator and chemoattractant for neutrophils involved in tumor progression in various cancer types (73–79). It was the hub gene in bladder urothelial carcinoma (BLCA), LUSC, and THCA, regulating the modules associated with response to molecules of bacterial origin, extracellular structure organization, cellular response to biotic stimulus, and cell chemotaxis. These results further proved that it might be a risk factor for cancer progression due to the immunosuppressive effect on the tumor microenvironment.

We have observed that *CXCL2*, *NR4A1* and *TIPRL* are expressed at lower levels in tumor tissues compared to normal tissues, but survival analyses point to high expression of these genes as a risk factor for survival in tumor patients (Figure 5F, G and I). This is supported by another study on the prognostic significance and mechanisms of *CXCL* genes (80), which also identified lower expression of *CXCL2* in LUSC tumor tissue and higher HR. A similar phenomenon has been observed for TP53 in tumor biology, where TP53 is lowly expressed as a tumor suppressor gene in tumor patients, but mutants of TP53 are highly expressed and pro-oncogenic in tumor patients (81). The three risk genes we identified, *CXCL2*, *NR4A1* and *TIPRL* are also even known to be functionally related to TP53 in tumor biology (80). We believe that this complex mechanism of tumor biology is the result of multiple regulatory mechanisms, and our discovery of the role of TFEB reveals the hidden regulatory layer and provides new insights.

However, the increase of *NR4A1* and *HIST1H1E/H1-4* mRNA levels might not be regulated by TFEB but due to the stress response. It implies that environmental stresses are more critical for regulating their expressions. Here, our findings provide a broader range of references of more TFEB downstream targets responding to three stimuli that might be crucial to cancer treatment.

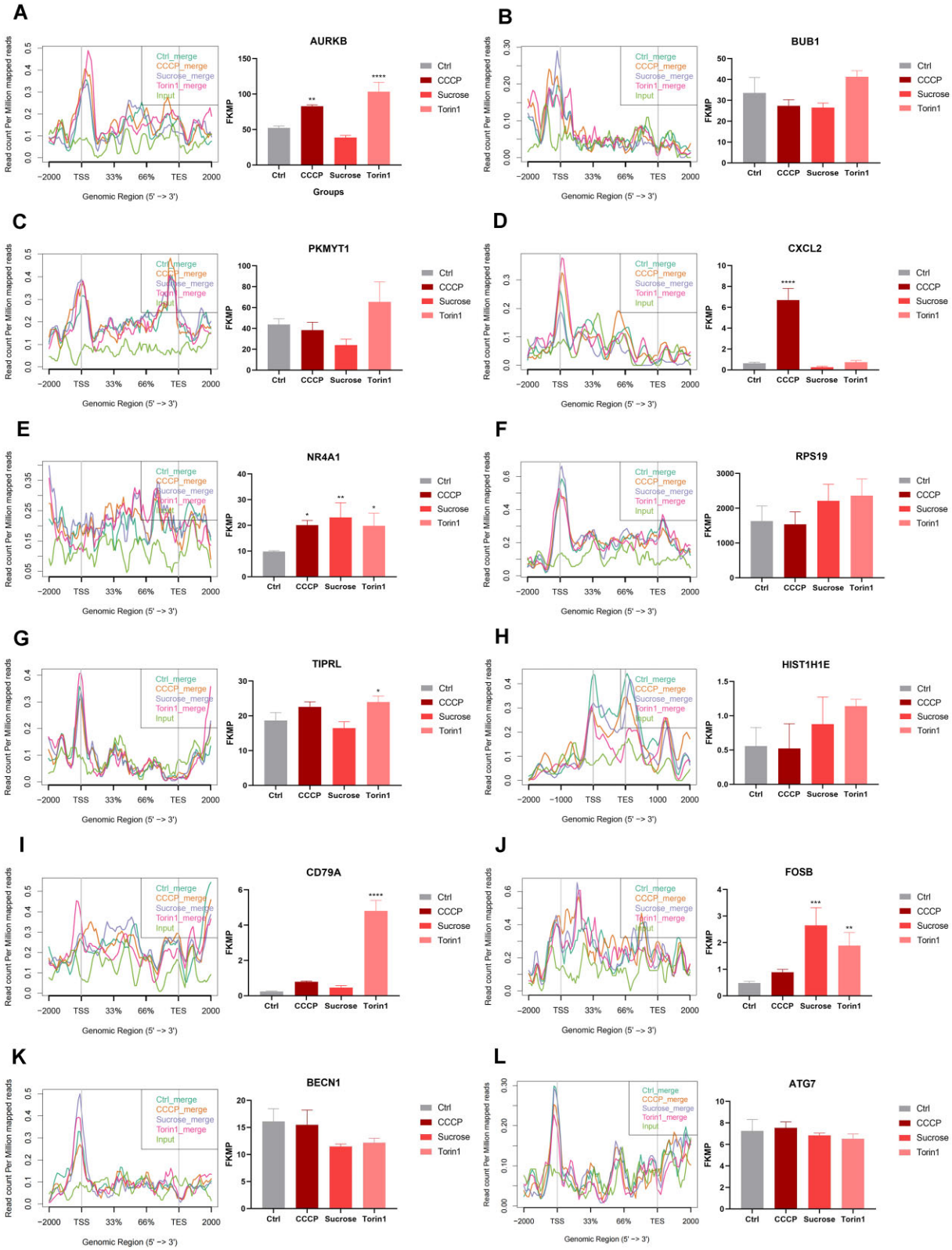

Figure 6. Average profiles of peak enrichment in gene body regions and mRNA levels of nine TFEB targets. The Dunnett's multiple comparison test was performed after analysis of variance (ANOVA). $^{*}P < 0.05$, $^{**}P < 0.01$, $^{***}P < 0.001$, $^{****}P < 0.0001$.

As a transcription factor, the different activities of TFEB in tumor cells or cells in TME might contribute to the diverse expression levels of these TFEB downstream targets in tumor tissues along with various prognoses. The subcellular translocation and activity of TFEB are mainly regulated by post-translational modifications (PTMs), such as phosphorylation and acetylation (82). The most well-reported form of the PTMs of TFEB is phosphorylation. We assessed the total protein and phosphorylated protein levels of TFEB from CPTAC through the UACLAN database (48,49). The decrease of phosphorylated TFEB in cancers might contribute to the high expression of its targets. Furthermore, other factors can also result in the diversities of the gene expressions in different cancers, such as the potential co-factors for TFEB, and the modification and splicing of pre-mRNAs (83–86). These complicated mechanisms are still needed to be further explored.

Another interesting phenomenon we observed in this study is that TFEB is not a hub gene, yet it significantly influences hub genes of pan-cancer modules. In our study, the MEGENA analysis is based on the transcriptomic data. However, as an important transcription factor regulating the autophagy-lysosomal pathway, TFEB exerts its effects mainly relying on the PTMs, e.g. phosphorylation, and acetylation (82,87), and subcellular translocation, rather than its transcriptomic level. Therefore, it is reasonable that TFEB is not the hub gene based on transcriptomic data, but it can regulate the mRNA expression levels of hub genes. It indicates that TFEB might work as a hidden player regulating the gene co-expression networks in Pan-cancer through regulation from other omics layers.

In summary, we provide a comprehensive reference for the TFEB downstream targets responding to three stresses and the dual roles of TFEB and its targets in cancer. TFEB, as a hidden player, can regulate expressions of various targets, some of which are risk factors, such as *CXCL2*, *PKMYT1* and *BUB1*, associated with cell cycle and immunosuppression. At the same time, some of these are protective factors, such as *CD79A*, related to the activation of T cells and increasing B cell infiltration in TME. Noteworthily, apart from *CXCL2*, which is included in the GSEA database as a TFEB target, other genes are novelly identified as TFEB targets through our experiments. We identified 1712 novel TFEB targets under three different cellular stresses in total. Among them, 111 novel TFEB targets were hub genes of conserved Pan-cancer modules. These TFEB targets are involved in multiple cellular pathways related to tumor development, prognosis and treatment. The dual function of TFEB targets may be cancer stage-dependent or TME-dependent, emphasizing the importance of stage-dependent treatment strategies. Our study helps to provide more clues for the pharmacological or genetic strategies to inhibit tumor growth, immunosuppression, and drug resistance, through regulating TFEB or TFEB targets. Many of the previous pan-cancer studies have been based on conclusions derived from the transcriptome and genome levels. Our study shows that at the epigenetic level, transcription factors are also actively involved in tumor biology, forming a hidden layer of regulation. However, our study still has limitations. We only integrated our experimental data from RNA-seq and ChIP-seq with pan-cancer gene co-expression networks reported in a previous study, which only showed survival analysis for the module prognosis analysis. More clinical data should be considered for the interpretation of TFEB target roles. In summary, TFEB targets are promising anticancer targets but warrant further exploration due to their multi-function.

Data availability

The expression profiles and ChIP-seq binding profiles of regulatory targets of TFEB under three different stress scenarios can be found in Shinyapp (https://minglab.shinyapps.io/shiny_pro/). For the TFEB binding sites from the ChIP-seq data, we further created a relevant session of the UCSC genome browser (https://genome.ucsc.edu/s/c6ming2/TFEB.PanCancer). The raw data of RNA-seq and ChIP-seq are available from the GEO. The RNA-seq GEO accession number is GSE273702, while the ChIP-seq GEO accession number is GSE273703. The data of MEGENA co-expression networks in 32 cancer types used here are available from the previous study by Xu and Zhang (36). All data have been included in the manuscript, figures, and supplemental data.

Supplementary data

Supplementary Data are available at NAR Cancer Online.

Acknowledgements

This work was performed in part at the High Performance Computing Cluster (HPCC) which is supported by the Information And Communication Technology Office (ICTO) of the University of Macau. We would like to thank Dr Shichao He for his figure layouts.

Author contributions: C.M., J.H. Lu and N.Y. Shao designed and supervised the study. J.F. Luo contributed to the RNA-seq and ChIP-seq experiments, data analysis and manuscript writing. S.J. Wang contributed to the survival tests. J.J. Fu constructed the Shinyapp website. P. Xu provided the data from gene co-expression networks in pan-cancer. All authors reviewed and revised the manuscript. J.F. Luo wrote the first draft of the manuscript, which all authors reviewed and edited. All the authors agreed to submit the published version of the manuscript.

Funding

National Natural Science Foundation of China [82271455]; University of Macau internal grant [SRG2023-00003-FHS, SRG2019-00177-FHS, MYRG-GRG2024-00272-FHS, MYRG-GRG2024-00273-FHS]; Dr Stanley Ho Medical Development Foundation [SHMDF-OIRFS/2024/002]; Guangdong Basic and Applied Basic Research Foundation [2022A1515012416]; Science and Technology Development Fund (FDCT) of Macau [FDCT/005/2023/SKL, FDCT/0025/2022/A1, FDCT/0010/2023/AKP, FDCT/0004/2021/AKP, FDCT/0038/2020/AFJ]; Southeast University Interdisciplinary Research Program for Young Scholars [2024FGC1004].

Conflict of interest statement

None declared.

References

1. Mizushima,N. (2007) Autophagy: process and function. *Genes Dev.*, **21**, 2861–2873.
2. Debnath,J., Gammoh,N. and Ryan,K.M. (2023) Autophagy and autophagy-related pathways in cancer. *Nat. Rev. Mol. Cell Biol.*, **24**, 560–575.

3. Qu,X., Yu,J., Bhagat,G., Furuya,N., Hibshoosh,H., Troxel,A., Rosen,J., Eskelinen,E.-L., Mizushima,N., Ohsumi,Y., *et al.* (2003) Promotion of tumorigenesis by heterozygous disruption of the beclin 1 autophagy gene. *J. Clin. Invest.*, **112**, 1809–1820.
4. Peng,Y., Miao,H., Wu,S., Yang,W., Zhang,Y., Xie,G., Xie,X., Li,J., Shi,C., Ye,L., *et al.* (2016) ABHD5 interacts with BECN1 to regulate autophagy and tumorigenesis of colon cancer independent of PNPLA2. *Autophagy*, **12**, 2167–2182.
5. Chen,J., Cai,S., Gu,T., Song,F., Xue,Y. and Sun,D. (2021) MiR-140-3p impedes gastric cancer progression and metastasis by regulating BCL2/BECN1-mediated autophagy. *Onco Targets Ther.*, **14**, 2879–2892.
6. Wijshake,T., Zou,Z., Chen,B., Zhong,L., Xiao,G., Xie,Y., Doench,J.G., Bennett,L. and Levine,B. (2021) Tumor-suppressor function of Beclin 1 in breast cancer cells requires E-cadherin. *Proc. Natl. Acad. Sci. U.S.A.*, **118**, e2020478118.
7. Long,J.S., Kania,E., McEwan,D.G., Barthet,V.J.A., Brucoli,M., Ladds,M.J.G.W., Nössing,C. and Ryan,K.M. (2022) ATG7 is a haploinsufficient repressor of tumor progression and promoter of metastasis. *Proc. Natl. Acad. Sci. U.S.A.*, **119**, e2113465119.
8. Li,X., He,S. and Ma,B. (2020) Autophagy and autophagy-related proteins in cancer. *Mol. Cancer*, **19**, 12.
9. Xia,H., Green,D.R. and Zou,W. (2021) Autophagy in tumour immunity and therapy. *Nat. Rev. Cancer*, **21**, 281–297.
10. Yamamoto,K., Venida,A., Yano,J., Biancur,D.E., Kakiuchi,M., Gupta,S., Sohn,A.S.W., Mukhopadhyay,S., Lin,E.Y., Parker,S.J., *et al.* (2020) Autophagy promotes immune evasion of pancreatic cancer by degrading MHC-I. *Nature*, **581**, 100–105.
11. Kauffman,E.C., Ricketts,C.J., Rais-Bahrami,S., Yang,Y., Merino,M.J., Bottaro,D.P., Srinivasan,R. and Linehan,W.M. (2014) Molecular genetics and cellular features of TFE3 and TFEB fusion kidney cancers. *Nat. Rev. Urol.*, **11**, 465–475.
12. Ladanyi,M., Lui,M.Y., Antonescu,C.R., Krause-Boehm,A., Meindl,A., Argani,P., Healey,J.H., Ueda,T., Yoshikawa,H., Meloni-Ehrig,A., *et al.* (2001) The der(17)t(X;17)(p11;q25) of human alveolar soft part sarcoma fuses the TFE3 transcription factor gene to ASPL, a novel gene at 17q25. *Oncogene*, **20**, 48–57.
13. Napolitano,G. and Ballabio,A. (2016) TFEB at a glance. *J. Cell Sci.*, **129**, 2475–2481.
14. Raben,N. and Puertollano,R. (2016) TFEB and TFE3: linking lysosomes to cellular adaptation to stress. *Annu. Rev. Cell Dev. Biol.*, **32**, 255–278.
15. Marchand,B., Arsenault,D., Raymond-Fleury,A., Boisvert,F.-M. and Boucher,M.-J. (2015) Glycogen synthase kinase-3 (GSK3) inhibition induces prosurvival autophagic signals in Human pancreatic cancer cells. *J. Biol. Chem.*, **290**, 5592–5605.
16. Giatromanolaki,A., Kalamida,D., Sivridis,E., Karagounis,I.V., Gatter,K.C., Harris,A.L. and Koukourakis,M.I. (2015) Increased expression of transcription factor EB (TFEB) is associated with autophagy, migratory phenotype and poor prognosis in non-small cell lung cancer. *Lung Cancer*, **90**, 98–105.
17. Liu,X., Yin,M., Dong,J., Mao,G., Min,W., Kuang,Z., Yang,P., Liu,L., Zhang,N. and Deng,H. (2021) Tubeimoside-1 induces TFEB-dependent lysosomal degradation of PD-L1 and promotes antitumor immunity by targeting mTOR. *Acta Pharm. Sin B*, **11**, 3134–3149.
18. Bellese,G., Tagliatti,E., Gagliani,M.C., Santamaria,S., Arnaldi,P., Falletta,P., Rusmini,P., Matteoli,M., Castagnola,P. and Cortese,K. (2023) Neratinib is a TFEB and TFE3 activator that potentiates autophagy and unbalances energy metabolism in ERBB2+ breast cancer cells. *Biochem. Pharmacol.*, **213**, 115633.
19. Takla,M., Keshri,S. and Rubinsztein,D.C. (2023) The post-translational regulation of transcription factor EB (TFEB) in health and disease. *EMBO Rep.*, **24**, e57574.
20. Easton,J.B. and Houghton,P.J. (2006) mTOR and cancer therapy. *Oncogene*, **25**, 6436–6446.
21. Bonam,S.R., Wang,F. and Muller,S. (2019) Lysosomes as a therapeutic target. *Nat. Rev. Drug Discov.*, **18**, 923–948.
22. O'Malley,J., Kumar,R., Inigo,J., Yadava,N. and Chandra,D. (2020) Mitochondrial stress response and cancer. *Trends Cancer*, **6**, 688–701.
23. Winter,J.M., Yadav,T. and Rutter,J. (2022) Stressed to death: mitochondrial stress responses connect respiration and apoptosis in cancer. *Mol. Cell*, **82**, 3321–3332.
24. Sardiello,M., Palmieri,M., Ronza,A.d., Medina,D.L., Valenza,M., Gennarino,V.A., Malta,C.D., Donaudy,F., Embrione,V., Polishchuk,R.S., *et al.* (2009) A gene network regulating lysosomal biogenesis and function. *Science*, **325**, 473–477.
25. Palmieri,M., Impey,S., Kang,H., di Ronza,A., Pelz,C., Sardiello,M. and Ballabio,A. (2011) Characterization of the CLEAR network reveals an integrated control of cellular clearance pathways. *Hum. Mol. Genet.*, **20**, 3852–3866.
26. Thoreen,C.C., Kang,S.A., Chang,J.W., Liu,Q., Zhang,J., Gao,Y., Reichling,L.J., Sim,T., Sabatini,D.M. and Gray,N.S. (2009) An ATP-competitive mammalian target of rapamycin inhibitor reveals rapamycin-resistant functions of mTORC1. *J. Biol. Chem.*, **284**, 8023–8032.
27. Kwon,K.-Y., Viollet,B. and Yoo,O.J. (2011) CCCP induces autophagy in an AMPK-independent manner. *Biochem. Biophys. Res. Commun.*, **416**, 343–348.
28. Ivankovic,D., Chau,K.-Y., Schapira,A.H.V. and Gegg,M.E. (2016) Mitochondrial and lysosomal biogenesis are activated following PINK1/parkin-mediated mitophagy. *J. Neurochem.*, **136**, 388–402.
29. Zhang,X., Cheng,X., Yu,L., Yang,J., Calvo,R., Patnaik,S., Hu,X., Gao,Q., Yang,M., Lawas,M., *et al.* (2016) MCOLN1 is a ROS sensor in lysosomes that regulates autophagy. *Nat. Commun.*, **7**, 12109–12109.
30. Langfelder,P. and Horvath,S. (2008) WGCNA: an R package for weighted correlation network analysis. *BMC Bioinf.*, **9**, 559.
31. Song,W.-M. and Zhang,B. (2015) Multiscale embedded gene Co-expression Network analysis. *PLoS Comput. Biol.*, **11**, e1004574.
32. Liu,W., Li,L. and Li,W. (2014) Gene co-expression analysis identifies common modules related to prognosis and drug resistance in cancer cell lines. *Int. J. Cancer*, **135**, 2795–2803.
33. Ruffalo,M., Koyutürk,M. and Sharan,R. (2015) Network-based integration of disparate omic data to identify "silent players" in cancer. *PLoS Comput. Biol.*, **11**, e1004595.
34. Ghanbari Maman,L., Palizban,F., Fallah Atanaki,F., Elmi Ghiasi,N., Ariaeenejad,S., Ghaffari,M.R., Hosseini Salekdeh,G. and Kavousi,K. (2020) Co-abundance analysis reveals hidden players associated with high methane yield phenotype in sheep rumen microbiome. *Sci. Rep.*, **10**, 4995.
35. Shafaroudi,A.M., Sharifi-Zarchi,A., Rahmani,S., Nafissi,N., Mowla,S.J., Lauria,A., Oliviero,S. and Matin,M.M. (2021) Expression and function of C1orf132 long-noncoding RNA in breast cancer cell lines and tissues. *Int. J. Mol. Sci.*, **22**, 6768.
36. Xu,P. and Zhang,B. (2023) Multiscale network modeling reveals the gene regulatory landscape driving cancer prognosis in 32 cancer types. *Genome Res.*, **33**, 1806–1817.
37. Chen,S., Zhou,Y., Chen,Y. and Gu,J. (2018) fastp: an ultra-fast all-in-one FASTQ preprocessor. *Bioinformatics*, **34**, i884–i890.
38. Kim,D., Paggi,J.M., Park,C., Bennett,C. and Salzberg,S.L. (2019) Graph-based genome alignment and genotyping with HISAT2 and HISAT-genotype. *Nat. Biotechnol.*, **37**, 907–915.
39. Pertea,M., Pertea,G.M., Antonescu,C.M., Chang,T.-C., Mendell,J.T. and Salzberg,S.L. (2015) StringTie enables improved reconstruction of a transcriptome from RNA-seq reads. *Nat. Biotechnol.*, **33**, 290–295.
40. Wickham,H. (2016) In: *ggplot2: Elegant Graphics for Data Analysis*. Springer-Verlag, NY.
41. Love,M.I., Huber,W. and Anders,S. (2014) Moderated estimation of fold change and dispersion for RNA-seq data with DESeq2. *Genome Biol.*, **15**, 550.

42. Chen,H. and Boutros,P.C. (2011) VennDiagram: a package for the generation of highly-customizable Venn and Euler diagrams in R. *BMC Bioinf.*, **12**, 35.
43. Zhou,Y., Zhou,B., Pache,L., Chang,M., Khodabakhshi,A.H., Tanaseichuk,O., Benner,C. and Chanda,S.K. (2019) Metascape provides a biologist-oriented resource for the analysis of systems-level datasets. *Nat. Commun.*, **10**, 1523.
44. Langmead,B., Trapnell,C., Pop,M. and Salzberg,S.L. (2009) Ultrafast and memory-efficient alignment of short DNA sequences to the human genome. *Genome Biol.*, **10**, R25.
45. Zhang,Y., Liu,T., Meyer,C.A., Eeckhoute,J., Johnson,D.S., Bernstein,B.E., Nusbaum,C., Myers,R.M., Brown,M., Li,W., *et al.* (2008) Model-based analysis of ChIP-Seq (MACS). *Genome Biol.*, **9**, R137.
46. Heinz,S., Benner,C., Spann,N., Bertolino,E., Lin,Y.C., Laslo,P., Cheng,J.X., Murre,C., Singh,H. and Glass,C.K. (2010) Simple combinations of lineage-determining transcription factors prime cis-regulatory elements required for macrophage and B cell identities. *Mol. Cell*, **38**, 576–589.
47. Shen,L., Shao,N., Liu,X. and Nestler,E. (2014) ngs.Plot: quick mining and visualization of next-generation sequencing data by integrating genomic databases. *Bmc Genomics [Electronic Resource]*, **15**, 284.
48. Chandrashekar,D.S., Bashel,B., Balasubramanya,S.A.H., Creighton,C.J., Ponce-Rodriguez,I., Chakravarthi,B.V.S.K. and Varambally,S. (2017) UALCAN: a portal for facilitating tumor subgroup gene expression and survival analyses. *Neoplasia*, **19**, 649–658.
49. Edwards,N.J., Oberti,M., Thangudu,R.R., Cai,S., McGarvey,P.B., Jacob,S., Madhavan,S. and Ketchum,K.A. (2015) The CPTAC Data Portal: a resource for cancer proteomics research. *J. Proteome Res.*, **14**, 2707–2713.
50. Subramanian,A., Tamayo,P., Mootha,V.K., Mukherjee,S., Ebert,B.L., Gillette,M.A., Paulovich,A., Pomeroy,S.L., Golub,T.R., Lander,E.S., *et al.* (2005) Gene set enrichment analysis: a knowledge-based approach for interpreting genome-wide expression profiles. *Proc. Natl. Acad. Sci. U.S.A.*, **102**, 15545–15550.
51. Lachmann,A., Xu,H., Krishnan,J., Berger,S.I., Mazloom,A.R. and Ma'ayan,A. (2010) ChEA: transcription factor regulation inferred from integrating genome-wide ChIP-X experiments. *Bioinformatics*, **26**, 2438–2444.
52. Huse,K., Bai,B., Hilden,V.I., Bollum,L.K., Våtsveen,T.K., Munthe,L.A., Smeland,E.B., Irish,J.M., Wälchli,S. and Myklebust,J.H. (2022) Mechanism of CD79A and CD79B support for IgM+ B cell fitness through B cell receptor surface expression. *J. Immunol.*, **209**, 2042–2053.
53. Wang,T., Qin,Y., Ye,Z., Jing,D.-S., Fan,G.-X., Liu,M.-Q., Zhuo,Q.-F., Ji,S.-R., Chen,X.-M., Yu,X.-J., *et al.* (2023) A new glance at autophagolysosomal-dependent or -independent function of transcriptional factor EB in human cancer. *Acta Pharmacol. Sin.*, **44**, 1536–1548.
54. Cui,Q., Wang,J.-Q., Assaraf,Y.G., Ren,L., Gupta,P., Wei,L., Ashby,C.R., Yang,D.-H. and Chen,Z.-S. (2018) Modulating ROS to overcome multidrug resistance in cancer. *Drug Resist. Updat.*, **41**, 1–25.
55. Srinivas,U.S., Tan,B.W.Q., Vellayappan,B.A. and Jeyasekharan,A.D. (2019) ROS and the DNA damage response in cancer. *Redox. Biol.*, **25**, 101084.
56. Senft,D. and Ronai,Z.E.A. (2016) Regulators of mitochondrial dynamics in cancer. *Curr. Opin. Cell Biol.*, **39**, 43–52.
57. Pu,J., Guardia,C.M., Keren-Kaplan,T. and Bonifacino,J.S. (2016) Mechanisms and functions of lysosome positioning. *J. Cell Sci.*, **129**, 4329–4339.
58. Martinez-Miguel,V.E., Lujan,C., Espie-Caullet,T., Martinez-Martinez,D., Moore,S., Backes,C., Gonzalez,S., Galimov,E.R., Brown,A.E.X., Halic,M., *et al.* (2021) Increased fidelity of protein synthesis extends lifespan. *Cell Metab.*, **33**, 2288–2300.
59. Dai,M., Yan,G., Wang,N., Daliah,G., Edick,A.M., Poulet,S., Boudreault,J., Ali,S., Burgos,S.A. and Lebrun,J.-J. (2021) In vivo genome-wide CRISPR screen reveals breast cancer vulnerabilities and synergistic mTOR/hippo targeted combination therapy. *Nat. Commun.*, **12**, 3055.
60. Havranek,O., Xu,J., Köhrer,S., Wang,Z., Becker,L., Comer,J.M., Henderson,J., Ma,W., Man Chun Ma,J., Westin,J.R., *et al.* (2017) Tonic B-cell receptor signaling in diffuse large B-cell lymphoma. *Blood*, **130**, 995–1006.
61. Julamanee,J., Terakura,S., Umemura,K., Adachi,Y., Miyao,K., Okuno,S., Takagi,E., Sakai,T., Koyama,D., Goto,T., *et al.* (2021) Composite CD79A/CD40 co-stimulatory endodomain enhances CD19CAR-T cell proliferation and survival. *Mol. Ther.*, **29**, 2677–2690.
62. Zou,J., Luo,C., Xin,H., Xue,T., Xie,X., Chen,R. and Zhang,L. (2022) The role of tumor-infiltrating B cells in the tumor microenvironment of hepatocellular carcinoma and its prognostic value: a bioinformatics analysis. *J. Gastrointest. Oncol.*, **13**, 1959–1966.
63. Bolanos-Garcia,V.M. and Blundell,T.L. (2011) BUB1 and BUBR1: multifaceted kinases of the cell cycle. *Trends Biochem. Sci*, **36**, 141–150.
64. Nie,M., Wang,Y., Yu,Z., Li,X., Deng,Y., Wang,Y., Yang,D., Li,Q., Zeng,X., Ju,J., *et al.* (2020) AURKB promotes gastric cancer progression via activation of CCND1 expression. *Aging (Albany NY)*, **12**, 1304–1321.
65. Zhang,Q.-Y., Chen,X.-Q., Liu,X.-C. and Wu,D.-M. (2020) PKMYT1 Promotes gastric cancer cell proliferation and apoptosis resistance. *Onco Targets Ther.*, **13**, 7747–7757.
66. Luan,M., Shi,S.-S., Shi,D.-B., Liu,H.-T., Ma,R.-R., Xu,X.-Q., Sun,Y.-J. and Gao,P. (2020) TIPRL, a novel tumor suppressor, suppresses cell migration, and invasion through regulating AMPK/mTOR signaling pathway in gastric cancer. *Front. Oncol.*, **10**, 1062.
67. Jeon,S.-J., Ahn,J.-H., Halder,D., Cho,H.-S., Lim,J.-H., Jun,S.Y., Lee,J.-J., Yoon,J.-Y., Choi,M.-H., Jung,C.-R., *et al.* (2019) TIPRL potentiates survival of lung cancer by inducing autophagy through the eIF2α-ATF4 pathway. *Cell Death. Dis.*, **10**, 959.
68. Jiang,N., Liao,Y., Wang,M., Wang,Y., Wang,K., Guo,J., Wu,P., Zhong,B., Guo,T. and Wu,C. (2021) BUB1 drives the occurrence and development of bladder cancer by mediating the STAT3 signaling pathway. *J. Exp. Clin. Cancer Res.*, **40**, 378.
69. Jin,W. and Ye,L. (2021) KIF4A knockdown suppresses ovarian cancer cell proliferation and induces apoptosis by downregulating BUB1 expression. *Mol Med. Rep.*, **24**, 516.
70. Gallo,D., Young,J.T.F., Fourtounis,J., Martino,G., Álvarez-Quilón,A., Bernier,C., Duffy,N.M., Papp,R., Roulston,A., Stocco,R., *et al.* (2022) CCNE1 amplification is synthetic lethal with PKMYT1 kinase inhibition. *Nature*, **604**, 749–756.
71. Szychowski,J., Papp,R., Dietrich,E., Liu,B., Vallée,F., Leclaire,M.-E., Fourtounis,J., Martino,G., Perryman,A.L., Pau,V., *et al.* (2022) Discovery of an orally bioavailable and selective PKMYT1 inhibitor, RP-6306. *J. Med. Chem.*, **65**, 10251–10284.
72. Li,M., Duan,X., Xiao,Y., Yuan,M., Zhao,Z., Cui,X., Wu,D. and Shi,J. (2022) BUB1 Is identified as a potential therapeutic target for pancreatic cancer treatment. *Front. Public Health*, **10**, 900853.
73. Lepsenyi,M., Algethami,N., Al-Haidari,A.A., Algaber,A., Syk,I., Rahman,M. and Thorlacius,H. (2021) CXCL2-CXCR2 axis mediates αv integrin-dependent peritoneal metastasis of colon cancer cells. *Clin. Exp. Metastasis*, **38**, 401–410.
74. Nie,S., Wan,Y., Wang,H., Liu,J., Yang,J., Sun,R., Meng,H., Ma,X., Jiang,Y. and Cheng,W. (2021) CXCL2-mediated ATR/CHK1 signaling pathway and platinum resistance in epithelial ovarian cancer. *J. Ovarian Res.*, **14**, 115.
75. Xu,X., Ye,L., Zhang,Q., Shen,H., Li,S., Zhang,X., Ye,M. and Liang,T. (2021) Group-2 innate lymphoid cells promote HCC progression through CXCL2-neutrophil-induced immunosuppression. *Hepatology*, **74**, 2526–2543.

76. Bao,Z., Zeng,W., Zhang,D., Wang,L., Deng,X., Lai,J., Li,J., Gong,J. and Xiang,G. (2022) SNAIL induces EMT and lung metastasis of tumours secreting CXCL2 to promote the invasion of M2-type immunosuppressed macrophages in colorectal cancer. *Int. J Biol. Sci.*, **18**, 2867–2881.
77. Cai,H., Chen,Y., Chen,X., Sun,W. and Li,Y. (2023) Tumor-associated macrophages mediate gastrointestinal stromal tumor cell metastasis through CXCL2/CXCR2. *Cell. Immunol.*, **384**, 104642.
78. Zhang,R., Dong,M., Tu,J., Li,F., Deng,Q., Xu,J., He,X., Ding,J., Xia,J., Sheng,D., *et al.* (2023) PMN-MDSCs modulated by CCL20 from cancer cells promoted breast cancer cell stemness through CXCL2-CXCR2 pathway. *Signal Transduct Target Ther.*, **8**, 97.
79. De Filippo,K., Dudeck,A., Hasenberg,M., Nye,E., van Rooijen,N., Hartmann,K., Gunzer,M., Roers,A. and Hogg,N. (2013) Mast cell and macrophage chemokines CXCL1/CXCL2 control the early stage of neutrophil recruitment during tissue inflammation. *Blood*, **121**, 4930–4937.
80. Shen,J., Wang,R., Chen,Y., Fang,Z., Tang,J., Yao,J., Gao,J., Chen,X. and Shi,X. (2023) Prognostic significance and mechanisms of CXCL genes in clear cell renal cell carcinoma. *Aging (Albany NY)*, **15**, 7974–7996.
81. Chen,X., Zhang,T., Su,W., Dou,Z., Zhao,D., Jin,X., Lei,H., Wang,J., Xie,X., Cheng,B., *et al.* (2022) Mutant p53 in cancer: from molecular mechanism to therapeutic modulation. *Cell Death. Dis.*, **13**, 974.
82. Zhang,J., Wang,J., Zhou,Z., Park,J.-E., Wang,L., Wu,S., Sun,X., Lu,L., Wang,T., Lin,Q., *et al.* (2018) Importance of TFEB acetylation in control of its transcriptional activity and lysosomal function in response to histone deacetylase inhibitors. *Autophagy*, **14**, 1043–1059.
83. Rambout,X., Dequiedt,F. and Maquat,L.E. (2018) Beyond transcription: roles of transcription factors in pre-mRNA splicing. *Chem. Rev.*, **118**, 4339–4364.
84. Mendel,M., Delaney,K., Pandey,R.R., Chen,K.-M., Wenda,J.M., Vågbø,C.B., Steiner,F.A., Homolka,D. and Pillai,R.S. (2021) Splice site m6A methylation prevents binding of U2AF35 to inhibit RNA splicing. *Cell*, **184**, 3125–3142.
85. Xu,J. and Richard,S. (2021) Cellular pathways influenced by protein arginine methylation: implications for cancer. *Mol. Cell*, **81**, 4357–4368.
86. Qu,J., Yan,H., Hou,Y., Cao,W., Liu,Y., Zhang,E., He,J. and Cai,Z. (2022) RNA demethylase ALKBH5 in cancer: from mechanisms to therapeutic potential. *J. Hematol. Oncol.*, **15**, 8.
87. Puertollano,R., Ferguson,S.M., Brugarolas,J. and Ballabio,A. (2018) The complex relationship between TFEB transcription factor phosphorylation and subcellular localization. *EMBO J.*, **37**, e98804.

Received: August 14, 2024. **Revised:** October 3, 2024. **Editorial Decision:** October 21, 2024. **Accepted:** October 28, 2024